Intelligent 3-D Sensing in Automated Manufacturing Processes

Q.M. Jonathan Wu and M.F. Ricky Lee
Vision and Sensing Group
National Research Council Canada
3250 East Mall, Vancouver, B.C.
Canada V6T 1W5
Email: Jonathan.Wu@nrc.ca

Clarence W. de Silva
Industrial Automation Laboratory
Department of Mechanical Engineering
University of British Columbia
Vancouver, B.C.
Canada V6T 1Z

Abstract:
This paper focuses on the design of an intelligent, three-dimensional (3-D) sensing system applying artificial intelligence methodologies for quality assurance in automated manufacturing processes. An efficient 3-D object-oriented knowledge base and reasoning algorithm is developed. The knowledge base includes knowledge concerning the products, manufacturing processes, and inspection methods. The products knowledge base contains properties design and manufacturing. The manufacturing and inspection knowledge bases include various manufacturing techniques, criteria for detection and diagnosis of defects, and standards and limitations on various decision-making actions. A fast and reliable assurance of product quality may be achieved through fault detection and diagnosis, using symbolic knowledge processing combined with numerical analysis of data. Incorporated with the reasoning algorithms, the knowledge base assists in the design process anticipating manufacturing problems and assuring specified end product properties. The knowledge base is regularly updated using feedback of the inspection results.

An inexpensive and accurate, non-contact 3-D range data measurement system is developed. In this system, multiple laser light stripes are projected onto the product and a single CCD camera is utilized to record the scene. The distortions in the projected line pattern are due to the orientation variations and surface curvature of the object. Utilizing a linear relation between the projected line distortion and surface depth, range data is recovered from a single camera image. The surface terrain information may be converted into the curvature, orientation, and depth of the shape to incorporate into the symbolic 3-D object-oriented knowledge base and reasoning algorithms.

1 Introduction

Automatic range sensing techniques have been intensively researched, particularly for applications in adaptive arc and laser welding, seam tracking, 3-D inspection and verification, surface and volumetric mapping, and robot guidance. Structured light approaches offer simplicity and low cost. Various patterns of structured light such as points, stripes, multiple stripes, dot matrix, and grids may be projected. Problems can arise, however, if the object has specular reflection.

Structured light-based whole field sensing techniques rely on low cost video technology, low power and an absence of signature (radar). Ranges generation is performed mainly by software, may be adapted to different working environments or robot modules.

Servo-Robot manufactures four families of line scan range sensors [1]. The M-spot and Jupiter families feature flying laser-spot technology which enables long depth of field (from 90 mm to 2000 mm). The BIP and SMART families result in a very high lateral measurement resolution (0.006-mm to 0.1 mm). The Lasiris manufactures several models of non-Gaussian (evenly illuminated) distinct structured beam line with a wavelength selection from 635 nm to 830 nm, output power of 1mW to 50mW, and the light pattern of parallel lines, dots, concentric circles, single line, dot matrix, single circle and cross hair [2].

Some research has been done by Saint-Marc *et al.*[3] using a PC-based scanner with a depth accuracy of 0.25 mm; and Archibald[4] using oscillating and rotating mirrors to swipe the laser beam over the object. The shape from a defocus method has been proposed by Nayar *et al.* [5] for a real-time range sensor.

The speed of the range finding techniques depends on the scanning method, signal acquisition time, and the depth construction algorithm. The accuracy depends on the scanning method and the camera parameter calibration. The resolution of the surface measurement depends on the scanning method.

0-7803-7078-3/01/$10.00 (C)2001 IEEE.

2 Structured Light Range Scanner

The structured light range scanner is based on the principle of triangulation (Figure 1). The process consists of illuminating an object from a known angle with a specific light pattern and observing the lateral position of the image to determine the depth information. The part is moved across the path of the projected light stripe. The distortion in the resulting line profiles can be translated into a depth profile of the part. By using this principle, we can analyze the original 2-D image to obtain 3-D information. Triangulation involves finding the linear relation between H (thickness of the object to be measured) in world coordinates and D_2 (offset of the laser stripe in image coordinate), as shown in Figure 1. The relation between H and D_1 (offset of the laser stripe in world coordinate), can be formulated as

$$H = \tan(\phi) \times D_1 \qquad (1)$$

The relation between D_1 and D_2 can be formulated by using a pin hole camera model, where W is the working distance and f is the optical focal length.

$$D_1 = \frac{W}{f} \times D_2 \qquad (2)$$

Substituting Equation 2 into Equation 1, a linear relationship between H and D_2 can be obtained:

$$H = \tan(\phi) \times \frac{W}{f} \times D_2 \qquad (3)$$

where W, f and ϕ are constants.

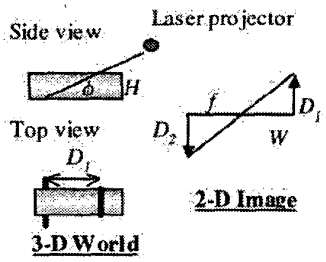

Figure 1. Triangulation Method.

3 Sensor Architecture

The experimental arrangement is sketched in Figure 2. The image is captured continuously through a PULNIX 6701 progressive scan camera, equipped with a 12.5 mm, f 1.4 Cosmicar TV lens, by a PCI frame grabber board, from Matrox Genesis. Single and multiple linear laser stripes generated from the LASIRIS laser diode structured-light projector of power 30 mW, and wavelength 670 nm, illuminate the object. The Microsoft Visual Basic 6.0 programming language is used as an objected oriented environment to develop the human machine interface and the Visual C++ 6.0 programming language is used to develop the algorithm as a DLL

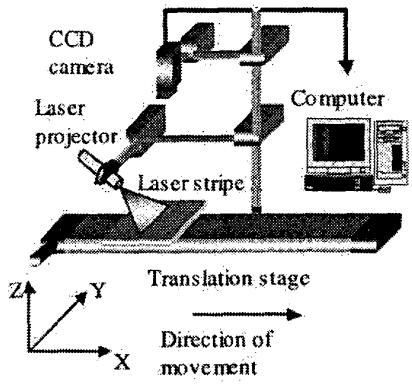

Figure 2. System Arrangement.

(Dynamic Link Library) in a DELL PC computer with a Pentium 400MHz microprocessor.

4. Knowledge-Based Fuzzy Approach

Fuzzy techniques have been successfully applied in various pattern recognition problems. The structure of the fuzzy approach presented in this paper is shown in Figure 3. Numerical data is obtained from a 2-D array of CCD sensors. Three main algorithms: stripe extraction, stripe coding and surface characterization have been developed. The stripe extraction is used to locate the stripe. The laser stripe's width varies from a single pixel to multiple pixels. Due to electronic noise, surface reflectance variation, and laser stripe diffusion around the surface of object, conventional thresholding techniques will either lose one laser stripe, or will produce a redundant edge. A simple peak finding technique finds more than one peak in a laser strip. To resolve this problem, a technique has been developed where a fuzzy reasoning engine is used for finding a local dominant peak. We can assume that the largest intensity profile change corresponds to the bounds of one stripe. Accordingly, the following criterion is applied when a line of intensity profile is scanned.

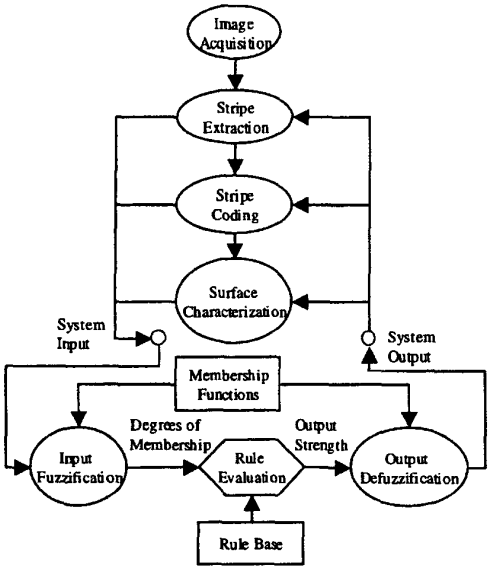

Figure 3. Structure of the Fuzzy System

4.1 Center Location

Five algorithms: Gaussian approximation, centre of mass, linear interpolation, parabolic estimator, and Blais and Rioux detector, have been reported by Trucco, et. Al., (1998) to determine the location of the stripe in an image, with sub-pixel accuracy. However, these algorithms are designed for a single stripe in the image, and are not applicable for multiple stripes. These methods use three highest, contiguous intensity values around the observed peak of the stripe to determine the sub-pixel accuracy of the observed peak. In the present section, a dominate peak finding method is developed to find peak to represent each group of pixels, then incorporated into the conventional algorithms, with modification, to achieve the sub-pixel accuracy.

1) Dominant Peak Locating

First, all maximum and minimum intensity pixels must be located at each scanning line from top to bottom. The dominant maximum has to be identified as a pixel point.

Step 1: Locate all global peak points $P_i^y, 0 \le i \le N_{peak}^y$ in row y, which meets the following condition:

$$\frac{f(x+\Delta x, y)-f(x,y)}{\Delta x} < 0 \text{ and } \frac{f(x,y)-f(x-\Delta x,y)}{\Delta x} \ge 0$$
$$\text{where } \Delta x = 1, 1 \le x \le M-2 \text{ and } 1 \le y \le N-2$$

Here i is the index of the individual peak point and N_{peak}^y represents the total number of peaks at row y. The peak points are the points in between either a rise or a flat intensity followed by a fall in intensity; e.g., P_1, P_2, P_3, etc. in Figure 4.

Step 2:

$$\frac{f(x+\Delta x, y)-f(x,y)}{\Delta x} \ge 0 \text{ and } \frac{f(x,y)-f(x-\Delta x,y)}{\Delta x} < 0$$
$$\text{where } \Delta x = 1, 1 \le x \le M-2 \text{ and } 1 \le y \le N-2$$

Locate all global valley points $V_i^y, 0 \le i \le N_{valley}^y$ in row y which meets the following condition; Here i is the index of the individual valley point and N_{valley}^y represents the total number of valley points at row y. The valley points are the points in between a fall in intensity followed by either a rise or a flat intensity; e.g., V_1, V_2, V_3, etc. in Figure 4.

Step 3: After all the maximum and minimum points have been located along each scanning line, it is required to locate the overall dominant peak among

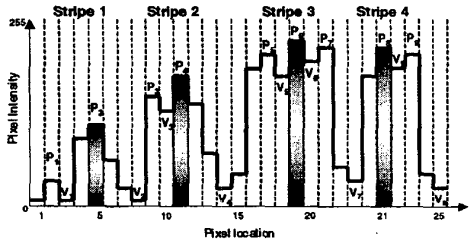

Figure 4. Artificial Intensity Histogram

all the maximum points located in Step 1. This dominant peak then represents the corresponding stripe group.

It is necessary to pick only one peak point and remove the redundant data points along each scanning line of laser strip. The searching rules given next represent the single-peak detector, which is used in each laser stripe group.

Check if there is any P_i^y between V_i^y and V_k^y which meet the peak location criterion. If the criterion is not satisfied then increase k until a peak is detected, where $1 \le i \le N_{peak}^y - 1$ and $i \le k \le N_{peak}^y$. If there are multiple peaks that meet the criterion, then chose the peak with highest intensity. Once the dominant peak is found between the two valleys, then set index

i equal to k and continue the search for the next dominant peak. The dominant that peak represents each laser stripe is found as

$DP_i^y, 0 \le i \le N^y_{dominant\ peak}$ according to:

$$DP_i^y : P_i^y \text{ if } f(P_i^y, y) - f(V_i^y, y) > threshold \text{ and } f(P_i^y, y) - f(V_k^y, y) > threshold \quad (4)$$

The *threshold* value has to be established experimentally. Two adjacent valleys have to be located as well, which envelope the dominant peak DP_i^y. These are found to meet the condition in (1). These two valleys are then set as the ROI^R and ROI^L according to

$$ROI_R{}^y = \{V_i^y \mid f(DP_i^y, y) - f(V_i^y, y) > threshold,\ DP_i^y > V_i^y, min\left|DP_i^y - V_i^y\right|\} \quad (5)$$

$$ROI_L{}^y = \{V_i^y \mid f(DP_i^y, y) - f(V_i^y, y) > threshold,\ DP_i^y < V_i^y, min\left|DP_i^y - V_i^y\right|\} \quad (6)$$

The regions of interest ROI^R and ROI^L will be used later as the right and left bounds to limit the data for the center calculation algorithms.
In Figure 7, three dominant peaks (DP) are located as P_2, P_5 and P_{10} which represent the 1st, 2nd and 3rd laser stripe groups and the region of interest (ROI^L, ROI^R) are found as (V_1, V_3), (V_4, V_6) and (V_7, V_{11}) which give the left and right bounding co-ordinates of the regions of interest, representing the 1st, 2nd, and 3rd laser stripe groups.

Consequently, it is now possible to refine the previous algorithms to calculate the centre of each laser stripe group independently.

4.2 Center of Mass Location

The traditional algorithm to compute the center of mass uses all the pixel points (x = 0 ~ 639) along the scanning lines (y). Only one peak will be obtained on each scanning line from y = 0 to y= 479. The weight average is computed as

$$P_{center}{}^y = \frac{\sum_{x=0}^{x=M-1}[f(x,y)\cdot x]}{\sum_{x=0}^{x=M-1} f(x,y)},\ 0 \le y \le N-1 \quad (7)$$

The image background contains a low intensity variation signal. If all the data are used in the center of mass calculation, then the background signals will introduce error. To improve the computational accuracy, the region of data points has to be limited to reflect the true laser stripe distribution. Two criteria may be applied to select the valid region of interest: by specific location of pixel points; and by specific intensity of pixel points.

To limit the region of computation specific location of pixel points, Trucco, *et al.* using the three, five and seven highest, contiguous intensity values around the observed peak. We use the P_i^y found from the dominant peak algorithm as presented before, as the observed peak in conjunction with two contiguous points $P_{i-1}{}^y$ and $P_{i+1}{}^y$ to calculate the center of mass, using (8). Another approach is to use ROI^L and ROI^R found from the dominant peak algorithm as the left and the right bounds of the region of interest shown in (9).

To limit the region of computation using the specific intensity of the pixel points either dynamic or constant thresholds values are selected to limit the region of interest for computation. The data points are screened with the intensity above this selected threshold value, as in equation (10) below.

$$p_{center}{}^y = \frac{\sum_{x=DP_{i-1}^y}^{x=DP_{i+1}^y}[f(x,y)\cdot x]}{\sum_{x=DP_{i-1}^y}^{x=DP_{i+1}^y} f(x,y)} \quad (8)$$

$$P_{center}{}^y = \frac{\sum_{x=ROI^L}^{x=ROI^R}[f(x,y)\cdot x]}{\sum_{x=ROI^L}^{x=ROI^R} f(x,y)},\ 0 \le y \le N-1 \quad (9)$$

$$P_{center}{}^y = \frac{\sum_{x=0}^{x=M-1}[f(x,y)\cdot x]}{\sum_{x=0}^{x=M-1} f(x,y)},\ 0 \le y \le N-1,\ f(x,y) \ge threshold \quad (10)$$

Linear Interpolation Approach
The approximate equation is

$$P_{center}{}^{y} = \begin{Bmatrix} DP_i{}^{y} - \dfrac{f(DP_{i+1}{}^{y},y) - f(DP_{i-1}{}^{y},y)}{2(f(DP_i{}^{y},y) - f(DP_{i-1}{}^{y},y))}, \\ f(DP_{i+1}{}^{y},y) > f(DP_{i-1}{}^{y},y) \\ DP_i{}^{y} - \dfrac{f(DP_{i+1}{}^{y},y) - f(DP_{i-1}{}^{y},y)}{2(f(DP_i{}^{y},y) - f(DP_{i+1}{}^{y},y))}, \\ f(DP_{i+1}{}^{y},y) < f(DP_{i-1}{}^{y},y) \end{Bmatrix} \quad (11)$$
$$, \ 0 \le y \le N-1$$

Parabolic Estimation Approach
The center of mass is computed according to

$$P_{center}{}^{y} = DP_i{}^{y} - \frac{f(DP_{i+1}{}^{y},y) - f(DP_{i-1}{}^{y},y)}{2[f(DP_{i+1}{}^{y},y) - 2f(DP_i{}^{y},y) + f(DP_{i-1}{}^{y},y)]} \quad (12)$$
$$, \ 0 \le y \le N-1$$

A gradient method is used to remove the redundant points on each line along the x-axis in a frame. If more than one data point lies in the same y-axis, the point with the closest gradient to the previous gradient is selected, and all others are removed. The discontinuity in pixels is also removed by checking the previous gradient

$$P_y^C = \{P_y^D : \min[(P_y^D - P_{y-1}^D), (P_{y-1}^D - P_{y-2}^D)], 2 < y < M\}$$

The forward and backward difference at specific pixel location can be formulated

The following fuzzy reasoning rules are used as a single peak detector among each laser stripe group.

Rule 1 A peak point belongs to a segment if its intensity is not very small and not very different from the neighborhood peak points.

Rule 2 If the gap between two peak points is very small, connect them into the current segment.

Rule 3 If a peak point's intensity is not very small, but is significantly different from those of the adjacent peak points, then the peak belongs to another segment.

Rule 4 If a segment is very short, then ignore it.

Rule 5 The center point of a peak is determined as roughly the point with an equal distance from the boundary valley points of the segment.

The rule evaluation is summarized as follows:

Rule 1: if A and B then Z and X
Rule 2: if C and D then Z and Y
Strength of Rule 1 = min(A, B)
Strength of Rule 2 = min(C, D)

X= Strength of Rule 1
Y= Strength of Rule 2
Z = Max(Strength of Rule 1, Strength of Rule 2)
= Max(min(A,B), min(C,D))

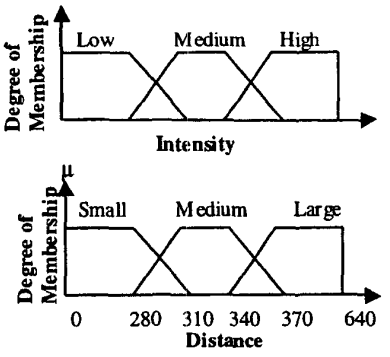

Figure 5. Fuzzy set for pixel intensity and distance .

Using the same fuzzy structure with different fuzzy description, membership function and rule, the approach can also be applied to the stripe coding and surface characterization. For stripe code, the rule base is summarized bellow:

Rule 1 A point belongs to a segment if its height is not very small and not very different from the neighborhood points.

Rule 2 If the gap is very small, group them into the current segment.

Rule 3 If the gap is very large and the heights at the boundary are similar then ignore it.

Rule 4 If a point's height is not very small, but considerably different from those of the adjacent point, then the points belongs to another segment.

Rule 5 If the segment is very short, then ignored it.

For surface characterization, the rule is summarized bellow:

Rule 1 If the curvature is not too large and the direction is uniformly downward then there may be a dent in the surface.

Rule 2 If the gap between two segments is not too large and the segments have similar height then it may represent a hole.

Rule 3 If the curvature is not too large and the direction is uniformly upward then there may be a bump in the surface.

5. Results and Discussion

The approach presented in this paper for sensing an object on a conveyor belt is tested with the following set-up parameters:

Sensor Element	648(H)×480(V)
Field of View	14-cm (H) ×10.5-cm (V)
Working Height	10 cm
Conveyor Speed	1 cm/sec

The performance achieved by the present approach is summarized below:

Lateral resolution (mm)	1.696±0.02
Scanned area (cm^2)	87.24±1.01
Depth range	0.44 mm to 7 cm
Depth resolution	0.22 mm
Profiling rate	4 cm^2/sec

Figure 7(a) and 7(b) shows an object illuminated with ambient light. Figure 7(c) and 7(d) shows an object illuminated with structured light. The stripe has successfully been extracted and coded into corresponding segments. The problems caused by electronic noise, surface reflectance variation, and laser stripe diffusion around the surface of the objects have been successfully solved by the fuzzy rule-based approach. The bump, hole and dent were identified, as shown in Figures 7(c) and 7(d). These initial results are promising because the total processing time for a depth image composed of 11 stripes did not exceed 4 second.

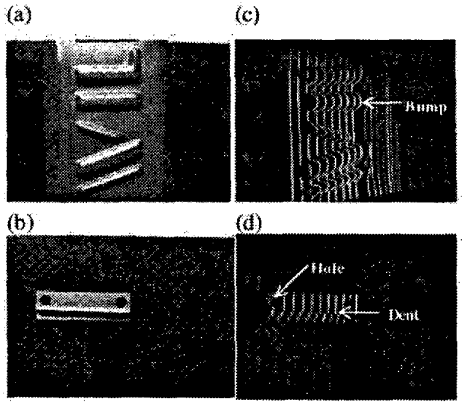

Figure 7. Examples.

The approach may fail if there is a very large height or intensity change in one object. Learning algorithms will be used to tune the fuzzy parameters and adding more rules to the knowledge base may be needed.

6. Conclusion

A rule-based approach was developed for automated 3-D sensing of data in manufacturing processes. Using a single 2-D CCD camera, laser structured light, and fuzzy techniques for rule-based decision making, it is possible to successfully interpret 3-D scenery. The lateral resolution depends on the conveying speed and time of camera capture, OS overhead, and bandwidth of data transfer. A higher resolution can be achieved by lowering the conveying speed. Lower resolution, as a result of increased profiling speed, can be achieved by controlling of the number of frames captured. The depth resolution can be adjusted by changing the working height, but higher depth resolution results in a lower profiling rate. We will also focus on the learning algorithms for tuning of the parameters of fuzzy logic decision systems, and solutions to the occlusion problems.

7. Reference

[1] Servo-Robot Inc., *User's Manual on Range Sensor*, 1380 Graham Bell, Boucherville, Quebec, Canada J4B 6H5, 1996

[2] LASIRIS Inc. *Literature on Laser Diode Structure Light Products*, Quebec, Canada H4R 2K3, 1998

[3] P. Saint-Marc, J. L. Jezouin, and G Medding,"A versatile PC-based range finding system", IEEE *Transactions on Robotics and Automation*, vol. 7, pp. 250-256, 1991.

[4] C. Archibald, "Robot wrist-mounted laser range finders and applications," Proceedings *of Electronic Imaging'90*, East Exposition and Conference, Boston, MA, 1990

[5] S.K. Nayar, M. Watanabe, and M. Noguchi, "Real-time focus range sensor," *Proceedings of IEEE International Conference on Computer Vision*, Cambridge, MA, pp. 995-1001, 1995.